SCIENCE LETTERS

ISSN: 1675-7785
eISSN: 2682-8626

Available online at
http://myjms.mohe.gov.my/index.php/sl

Science Letters 20(2) 2026, 257-264.

Science Letters

Influence of Chitosan Concentration on the Physicochemical and Electrochemical Properties of Glutaraldehyde-Crosslinked Flowable Chitosan Hydrogels for Electrode Coating Applications

Nurlily Marlissa Azmin[1], Dania Adila Ahmad Ruzaidi[1], Mohd Hafiz Md Ali[1], Siti Roha Ab Mutalib[1], Mohd Muzamir Mahat[1], Radin Siti Fazlina Nazrah Hirzin[1], Nur Aimi Jani[1,2,3*]

[1]*Faculty of Applied Sciences, Universiti Teknologi MARA Shah Alam, 40450, Shah Alam, Selangor, Malaysia*
[2]*Electrochemical Materials and Sensor (EMaS) Research Group, Faculty of Applied Sciences, Universiti Teknologi MARA Shah Alam, 40450, Shah Alam, Selangor, Malaysia*
[3]*Centre for Functional Materials and Nanotechnology, Universiti Teknologi MARA Shah Alam, 40450, Shah Alam, Selangor, Malaysia*

ARTICLE INFO

Article history:
Received 03 November 2025
Revised 15 April 2026
Accepted 15 April 2026
Published 30 Jun 2026

Keywords:
Chitosan hydrogels
Glutaraldehyde
Glacial acetic acid
Concentration
Electrode sensor applications

DOI:
10.24191/scl.v20i2.9399

ABSTRACT

Recently, chitosan-based hydrogels have gained attention for their biocompatibility, biodegradability and relevance as effective electrode coating for sensors. However, producing well-coating chitosan hydrogel through a facile process remains challenging. This study investigates the effect of chitosan concentration on the properties of glutaraldehyde-chitosan hydrogels for electrode coatings. Flowable hydrogels were produced via facile chemical crosslinking process under ambient condition, eliminating the need of heating or controlled atmospheres by dissolving chitosan powder with concentrations ranging from 1.0% to 5.0% (w/v) in distilled water, followed by addition of 1.2% v/v of glacial acetic acid and glutaraldehyde as crosslinker to form hydrogels for about 2 hours at room temperature. The hydrogels were characterized by rheological testing, Fourier transform infrared spectroscopy (FTIR), and electrochemical impedance spectroscopy (EIS). Results showed that the 3.0% w/v CS hydrogel demonstrating optimal viscosity of 9.15 Pa·s, while FTIR confirmed successful crosslinking by glutaraldehyde and glacial acetic acid within the hydrogel matrix. Furthermore, EIS indicated superior electrical conductance (3.25×10^{-3} S) for the 3.0% w/v CS hydrogel, confirming it as the optimal candidate that integrates physicochemical and electrochemical properties for electrode coatings, which supports efficient and reliable sensor device development.

* Corresponding author. *E-mail address*: *nuraimi_jani@uitm.edu.my*

https://doi.org/10.24191/scl.v20i2.9399

1. INTRODUCTION

Hydrogels, hydrophilic polymer networks have recently gained considerable attention for their high-water content, flexibility, biocompatibility, and ionic conductivity which are advantageous for biomedical and sensor applications (Revete et al., 2022; Shi et al., 2024). For instance, among natural polymers, chitosan (CS)-based hydrogels stand out and have attracted significant interest due to their biodegradability, biocompatibility, strong bio-adhesive properties, good injectability, strong network-forming capability and excellent gel-forming ability (Ramírez-Campas et al., 2025; Wu et al., 2023). These qualities enable CS hydrogels to serve as an effective candidate for electrode coatings where mechanical stability, chemical compatibility, and efficient ion transport are crucial.

Nonetheless, despite all these pros, contemporary challenges in hydrogel development involve optimizing viscosity for injectability, attaining uniform surface morphology, balancing chemical composition with electrical performance and securing effective chemical crosslinking with glutaraldehyde (GA) and glacial acetic acid (HAc). Overcoming these challenges is vital as to achieve the best performance of for hydrogel coatings in sensor applications.

There are several parameters that can crucially impact the optimization of hydrogel coating for sensor applications. For instance, the type and concentration of cross-linkers, presence of additives used in hydrogel formation, pH and temperature for hydrogel gelation and concentration of CS (Tahir et al., 2025). Among these parameters, the concentration of CS itself is mainly significant concerning the viscosity, chemical composition and ionic conductivity of the hydrogel. Meaning that, increasing the concentration of CS characteristically improves gel hardness and crosslinking density but may reduce conductance owing to the denser hydrogel matrix. Hence, optimizing the CS concentration is vital for modifying hydrogel properties to meet specific biomedical and sensor application requirements. The present work concentrates on the influence of CS concentration on the viscosity, chemical composition and electrochemical performance of CS-based hydrogels.

2. EXPERIMENTAL

Five flowable chitosan (CS) hydrogels with different concentrations of CS powder (≥90% deacetylation degree and low molecular weight of 10-20 kDa, Bio Basic Inc., Markham, Ontario, Canada) ranging from 1.0% to 5.0% (w/v) were produced by initially dissolved the powder in distilled water for 30 minutes, followed by the addition with 1.2% v/v of HAc (≥99%, Sigma-Aldrich, Merck KGaA, Darmstadt, Germany) without further dilution and stirred for 1 hour. Then, a dropwise of 1.0% v/v of GA (50% photographic grade, Sigma-Aldrich, Merck KGaA, Darmstadt, Germany) was added and the mixture was stirred for another 30 minutes. The stirring process was carried out utilizing a magnetic hotplate stirrer (Model SH-2 Joanlab, Zhejiang, China) at 450 rpm at room temperature (RT). Upon completion of the 2-hour stirring period, flowable hydrogel was kept under RT prior to subsequent use (Galan et al., 2021; Alimirzaei et al., 2017). Five hydrogel formulations with concentrations of 1.0%, 2.0%, 3.0%, 4.0%, and 5.0% were subjected to rheological, FTIR, and EIS analyses. For each formulation, measurements were repeated three times on the same sample to ensure measurement reproducibility.

3. RESULTS AND DISCUSSIONS

3.1 Rheological Testing

A rheological testing was conducted to evaluate the viscous properties of the flowable CS hydrogels for electrode coating. As shown in **Fig. 1**, viscosity decreased with increasing shear rate, indicating typical shear-thinning behavior (Saberi et al., 2025). This indicated that these flowable hydrogels possessed non-Newtonian shear-thinning fluid behaviour (Li et al., 2025). Shear-thinning is advantageous for electrode

https://doi.org/10.24191/scl.v20i2.9399

coating, as it facilitates flow under applied stress while allowing structural recovery after deposition through reversible crosslinking. Improved shear-thinning behavior enhances injectability and coating adhesion to the electrode surface.

As summarized in Table 1, viscosity increased with CS concentration, showing a monotonic concentration-dependent trend with shear-thinning onset observed at ~10 s^{-1}, thereby influencing formulation suitability for electrode coating (Tian et al., 2025). At low-shear viscosity plateau (~5 s^{-1}), the 1.0% and 2.0% w/v formulations showed low viscosities (2.01 and 5.02 Pa·s) and correspondingly low shear stresses (10.05 and 25.10 Pa). This low resistance to deformation may weaken cohesion during deposition and reduce coating stability on the electrode surface. Conversely, the 4.0% and 5.0% w/v formulations produced higher viscosities and corresponding shear stresses (72.55 and 91.55 Pa), indicating greater resistance to flow. Although stability may improve, higher stress can increase the required extrusion force and hinder uniform coating spreading. Previous studies on direct-ink writing and polymer inks highlight the need for balanced rheology during deposition (Sauret et al., 2026). Shear-thinning facilitates flow, whereas yield stress and viscoelasticity preserve post-deposition stability. Sauret et al. (2026) reported that high flow resistance requires greater extrusion pressure, increasing the risk of nozzle clogging or particle jamming. In contrast, low resistance may cause excessive spreading and poor structural integrity. Thus, a moderate viscosity is preferred to ensure smooth coating and post-deposition film stability. In this context, the 3.0% w/v CS formulation offers balanced rheological behaviour for electrode coating.

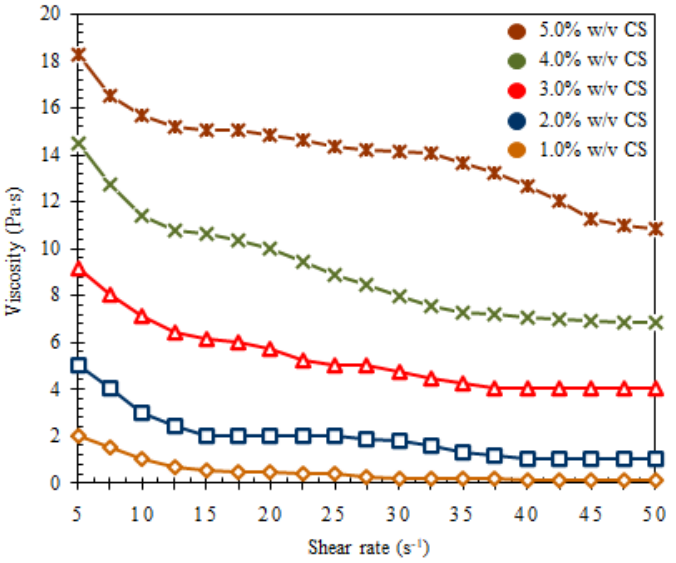

Fig. 1. The viscosity of flowable CS hydrogel with varying concentration of CS at 1.0% w/v CS, 2.0% w/v CS, 3.0% w/v CS, 4.0% w/v CS, and 5.0% w/v CS, displaying increased viscosity with increased content of CS

Table 1. The comparison of viscosity and shear stress change as a function of constant low shear rate between flowable chitosan (CS) hydrogels varied by the sample concentrations with shear-thinning onset observed at ~10 s^{-1}

Sample concentration	Viscosity at 5 s^{-1} (Pa·s)	Shear stress at 5 s^{-1} (Pa)
1.0% w/v CS	2.01	10.05
2.0% w/v CS	5.02	25.10
3.0% w/v CS	9.15	45.75
4.0% w/v CS	14.51	72.55
5.0% w/v CS	18.31	91.55

https://doi.org/10.24191/scl.v20i2.9399

3.2 FTIR Analysis

The FTIR spectra of the major peaks of flowable CS hydrogels varied by 5 different concentrations of CS have been depicted in **Fig. 2**a. The characteristic peak at 3250 cm^{-1} indicated the strong hydroxyl band present (O–H/N–H stretching) due to both intermolecular and intramolecular of hydrogen bonds (Cheng et al., 2026). Meanwhile, the peak at 1729 cm^{-1} corresponds to the carbonyl band (C=O stretching) of residual, non-reacted aldehyde groups from glutaraldehyde (GA). This suggests incomplete consumption of aldehyde groups during imine (C=N) formation in the Schiff base crosslinking process (Dacrory et al., 2024).

The FTIR spectra in **Fig. 2**b shows the characteristic peaks of optimized 3.0% w/v CS formulation, GA and, HAc. Both GA and 3.0% w/v CS exhibited a peak at 3250 cm^{-1} corresponding to O–H/N–H stretching vibration (Gan et al., 2024). A peak at approximately 3000 cm^{-1} is attributed to the C–H stretching of the methyl group present in the acid (Le & Hoang, 2026). GA also showed a peak at 1729cm^{-1} representing C=O stretching (Dacrory et al., 2024). The absorption band near 1630 cm^{-1} is attributed to C=N stretching (Schiff base linkage), formed via condensation reaction between aldehyde groups of GA and primary amine groups of CS. The peak at approximately 1396 cm^{-1} is assigned to CH_3 symmetric deformation (CH_3 bending), while, the band around peak 1250 cm^{-1} is attributed to C–N stretching of amine group. The presence and possible shift of these bands in the hydrogel spectrum indicated chemical interactions between CS and GA during hydrogel formation (Ortega-Sánchez et al., 2024). Hence, 3.0% w/v CS flowable hydrogel sample was selected as the optimized formulation as it exhibited a balanced spectral profile and suitable structural characteristics, suggesting adequate interaction with both GA and HAc under moderate conditions.

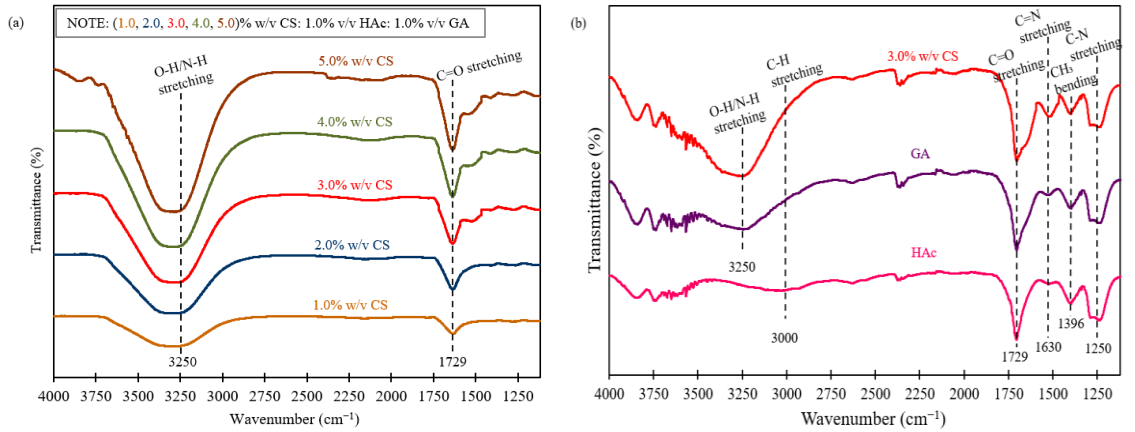

Fig. 2. The FTIR spectra of (a) flowable CS hydrogel varied by different concentration of CS with formulation of ((1.0, 2.0, 3.0, 4.0, 5.0) % w/v CS: 1.0% v/v HAc: 1.0% v/v GA) and (b) optimized flowable CS hydrogel with reference glutaraldehyde (GA) and glacial acetic acid (HAc)

3.3 EIS Analysis

The complex impedance plots of flowable CS hydrogel with varying concentration of CS with reference impedance plots of distilled water have been shown in Fig. 3a and Fig. 3b respectively. From the Nyquist plots shown in Fig. 3a and Fig. 3b, the impedance values corresponding to the resistive components of the system were ascertained by assessing the real axis intercept (*Z'*). Particularly, the high-frequency intercept denotes the solution resistance (*Rs*), considering the bulk ionic resistance of the hydrogel, meanwhile the low-frequency intercept reflecting the summation of the solution and polarization (charge transfer)

https://doi.org/10.24191/scl.v20i2.9399

resistance (*Rs* + *Rp*). Based on Table 2, specifically the flowable CS hydrogel that varied by its concentration from 1.0% w/v to 5.0% w/v, it is noted that, the impedance values decrease as the concentration of CS increases. This clearly happened due to increasing ionic conductivity with increasing CS concentration (Wang et al., 2025).

In addition, the fitted Randles circuit in the Nyquist plot in Fig. 3b displayed a representation of an electrode system that comprises of solution resistance (*Rs*), polarization (charge transfer) resistance (*Rp*) and constant phase element (CPE) which is also defined as non-ideal capacitor (Han et al., 2026). Hence, enables the extraction of key electrochemical parameters which confirms the electrode kinetics and electrocatalytic activity within the flowable CS hydrogel. The Nyquist plots depict an inclined region which suggested the diffusion-controlled process, yet the absence of Warburg element (*W*) in the fitting model indicates the diffusion effects are minimal or overlapped with capacitive behaviour represented by CPE. This phenomenon is typical considering the sample is flowable CS hydrogel, where ionic transport is influenced by the porous and hydrated network but rarely displays a clearly identifiable Warburg impedance within the frequency range examined. This is owing to the characteristic of hydrogels that are soft and often have variables or tricky-to-measure geometry, hence, many studies report conductance as a practical comparative measure rather than absolute conductivity (Daso et al., 2025; Singh et al., 2026).

The value of solution resistance (*Rs*) is directly attained from the fitting Nyquist plots and the formula of conductance bypasses the need for geometric parameters. The conductance can be determined by using following equation (Ariyoshi et al., 2022), see Equation (1):

$$G = \frac{1}{R} \tag{1}$$

As noted in Equation (1), *G* and *R* denote the conductance and resistance respectively, where *G* is conductance in siemens (S) and *R* is resistance in ohms (Ω). The relationship between resistance, conductivity and conductance are shown mathematically as in the following, see Equation (2):

$$R = \frac{L}{\kappa A} \tag{2}$$

where κ is the intrinsic conductivity, *L* is the distance between electrode and *A* is the cross-sectional area of the electrode. Conductance depends on both conductivities and geometry; hence the relationship is written as shown in following equation, see Equation (3):

$$G = \frac{1}{R} = \frac{L}{\kappa A} \tag{3}$$

Since the geometrical parameters are often challenging to be measured precisely in the hydrogel or solution samples, and the conductance is the reciprocal of resistance, hence it can be directly evaluated using Equation (1) where *R* is the solution resistance (*Rs*). As displayed in **Table 2**, it is interesting to note that the impedance level and conductance of distilled water vice versa with one another, which the impedance level is very high with lowest value of conductance compared to all those samples of flowable CS hydrogel. Distilled water has a very high impedance level owing to its extremely low concentration of ion (Yalamanchili, 2011).

Based on **Table 2**, the conductance of the hydrogel samples increased from 1.0% to 4.0% w/v CS as the Rs value decreased. However, at 5.0% w/v CS, the conductance slightly decreased despite the relatively low impedance. This may be attributed to the excessive viscosity of CS, which hinders ion mobility within the hydrogel matrix and reduces conductance (Chen et al., 2026; Zha et al., 2026). Although the 4.0% w/v CS sample exhibited slightly lower Rs and slightly higher conductance, the difference compared with the

https://doi.org/10.24191/scl.v20i2.9399

3.0% w/v CS formulation was minimal. Considering the electrochemical, rheological, and FTIR results, the 3.0% w/v CS hydrogel was selected as the most balanced formulation for electrode coating.

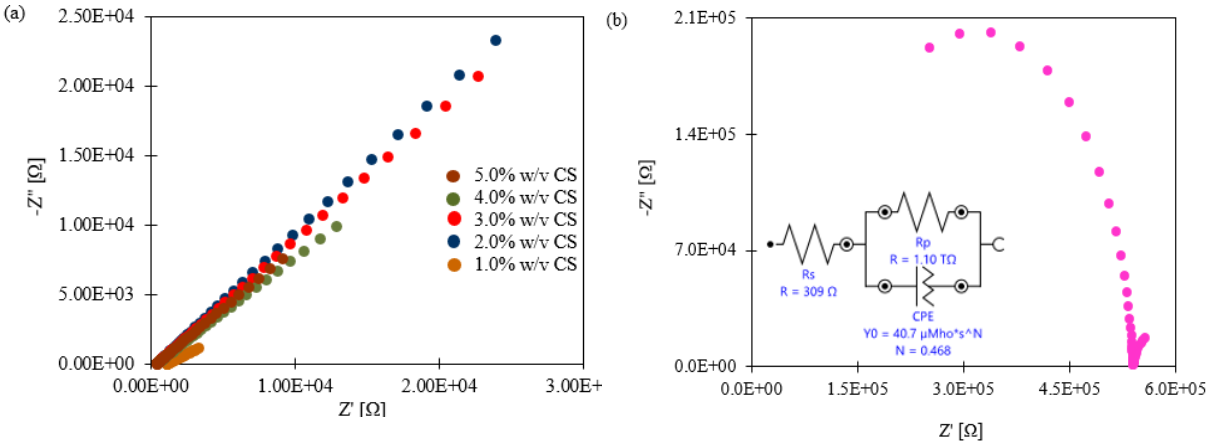

Fig. 3. The complex impedance plots of (a) flowable CS hydrogels with varying concentrations of CS and (b) reference impedance plot of distilled water

Table 2. The comparison of conductance between distilled water and flowable CS hydrogels varied by the sample concentrations

Sample concentration	Rs value (Ω)	Relative impedance level (based on Rs value)	Conductance, G (S)
Blank (distilled water)	1.19×10^{5}	Very high	8.42×10^{-6}
1.0% w/v CS	9.86×10^{2}	High	1.01×10^{-3}
2.0% w/v CS	3.48×10^{2}	Moderate	2.87×10^{-3}
3.0% w/v CS	3.08×10^{2}	Low	3.25×10^{-3}
4.0% w/v CS	3.07×10^{2}	Low	3.26×10^{-3}
5.0% w/v CS	3.16×10^{2}	Low	3.16×10^{-3}

4 CONCLUSION

In summary, the flowable CS hydrogel was successfully formed by chemical crosslinking process. The effects of CS concentration on hydrogel formation have been studied. The results shown by comprehensive characterization using rheology, FTIR and EIS analyses demonstrated that the flowable hydrogel with 3.0% w/v CS offers the most favourable conditions for hydrogel electrode coating. It shows effective crosslinking with both GA and HAc and has good viscosity of 9.15 Pa·s. Altogether, 3.0% flowable CS hydrogel offers excellent performance across all analyses with conductance value of 3.25×10^{-3} S. These integrated rheological, chemical and electrochemical properties make the 3.0% w/v CS hydrogel an ideal candidate for electrode coatings, providing efficient and reliable sensor device development.

Acknowledgement

The author gratefully acknowledges Universiti Teknologi MARA (UiTM) Shah Alam, Selangor, Malaysia and the Faculty of Applied Sciences, UiTM Shah Alam, Selangor, Malaysia, for their provision of facilities and financial support for this research.

https://doi.org/10.24191/scl.v20i2.9399

Conflict of Interest Statement

The author confirms that this research was carried out in the absence of any personal gain, commercial or financial conflicts and declares absence of competing interests regarding the publication of this paper.

REFERENCES

Alimirzaei, F., Vasheghani-Farahani, E., Ghiaseddin, A., Soleimani, M., Pouri., & Najafi-Gharavi, Z. (2017). pH-Sensitive Chitosan Hydrogel with Instant Gelation for Myocardial Regeneration. *Journal of Tissue Science & Engineering*, *08*(03). https://doi.org/10.4172/2157-7552.1000212

Ariyoshi, K., Mineshige, A., Takeno, M., Fukutsuka, T., Abe, T., Uchida, S., & Siroma, Z. (2022). Electrochemical Impedance Spectroscopy Part 2: Applications. *Electrochemistry*, *90*(10), 102008. https://doi.org/ 10.5796/electrochemistry.22-66080

Chen, R., Guo, R., Li, Y., Yan, H., Huang, J., Xu, H., Shi, W., Zhang, Z., Zhuo, S., & Liu, M. (2026). Hydrogel ionic sensory systems. *Materials Chemistry Frontiers*, *10*(10), 1536–1572. https://doi.org/10.1039/d6qm00061d

Cheng, M., Lin, W., Yu, J., Gao, P., Shi, F., Wang, C., Ma, Y., Liu, Z., & Dong, G. (2026). A pH-triggered antibacterial and lubricating dual-function hydrogel coating for infection-resistant urinary catheters. *Frontiers in Bioengineering and Biotechnology*, *14*, 1–18. https://doi.org/10.3389/fbioe.2026.1751442

Dacrory, S., D'Amora, U., Longo, A., Hasanin, M. S., Soriente, A., Fasolino, I., Kamel, S., Al-Shemy, M. T., Ambrosio, L., & Scialla, S. (2024). Chitosan/cellulose nanocrystals/graphene oxide scaffolds as a potential pH-responsive wound dressing: Tuning physico-chemical, pro-regenerative and antimicrobial properties. *International Journal of Biological Macromolecules*, *278*, 134643. https://doi.org/10.1016/j.ijbiomac.2024.134643

Daso, R. E., Posey, R., Garza, H., Perry, A., Petersen, C., Fritz, A. C., Rivnay, J., & Tropp, J. (2025). Standardized Electrochemical Characterization of Conductive Hydrogels. *ChemRvix*. https://doi.org/10.26434/chemrxiv-2025-6n1bn

Galan, J., Trilleras, J., Zapata, P. A., Arana, V. A., & Grande-Tovar, C. D. (2021). Optimization of chitosan glutaraldehyde-crosslinked beads for reactive blue 4 anionic dye removal using a surface response methodology. *Life*, *11*(2), 1–20. https://doi.org/10.3390/life11020085

Gan, Z., Qi, R., Chen, B., Yuan, G., & Liao, M. (2024). Ultra-fast fabrication of MXene/PVA composite films through glutaraldehyde induced microgel framework. *Heliyon*, *10*(9). https://doi.org/10.1016/j.heliyon.2024.e30714

Han, T., Song, T., Gan, J., Han, D., & Niu, L. (2026). Frequency Dependence of Effective Capacitance Cec for Polyaniline Membrane-Based pH Sensor and its Extension to the Gouy–Chapman–Stern Model. *Electrochem*, *7*(2), 1–18. https://doi.org/10.3390/electrochem7020010

Le, A. H. Q., & Hoang, H. Y. (2026). From rice-husk waste to selective BTEX adsorbents: modified MWCNTs reveal a co-adsorption swing effect and improve field monitoring. *RSC Advances*, *16*, 8105–8118. https://doi.org/10.1039/d5ra08675b

Li, B., Huang, C., Wang, Z., Shi, Z., Xu, L., Huang, S., Qu, M., Xu, Z., Zhang, D., Guo, B., Liu, H., Liu, D., & Yao, P. (2025). Modeling of Extrusion 3D Bioprinting Precision Considering the Non-Newtonian Rheological Dynamics of Gelatin-Chitosan Hydrogels. *ACS Applied Polymer Materials*, *7*, 1257–1270. https://doi.org/10.1021/acsapm.4c02866

Ortega-Sánchez, C., Melgarejo-Ramírez, Y., Rodríguez-Rodríguez, R., Jiménez-Ávalos, J. A., Giraldo-Gomez, D. M., Gutiérrez-Gómez, C., Rodriguez-Campos, J., Luna-Bárcenas, G., Velasquillo, C., Martínez-López, V., & García-Carvajal, Z. Y. (2024). Hydrogel Based on Chitosan/Gelatin/Poly (Vinyl Alcohol) for In Vitro Human Auricular Chondrocyte Culture. *Polymers*, *16*(4), 1–19. https://doi.org/10.3390/polym16040479

Ramírez-Campas, U., P. Aubourg, S., Torres-Arreola, W., Plascencia-Jatomea, M., & Ezquerra-Brauer, J. M. (2025). Physical and Structural Properties of Chitosan–Squid Gelatin Hydrogels. *Gels*, *11*(2), 109 (article). https://doi.org/10.3390/gels11020109

https://doi.org/10.24191/scl.v20i2.9399

Revete, A., Aparicio, A., Cisterna, B. A., Revete, J., Luis, L., Ibarra, E., Segura González, E. A., Molino, J., & Reginensi, D. (2022). Advancements in the Use of Hydrogels for Regenerative Medicine: Properties and Biomedical Applications. *International Journal of Biomaterials*, *2022*. https://doi.org/10.1155/2022/3606765

Saberi, J., Karimzadeh, F., Varshosaz, J., & Labbaf, S. (2025). Shear-thinning conductive chitosan-based nano-hybrid hydrogels by host–guest supramolecular assembled poly ethylene glycol and reduced graphene oxide dual cross-linkers. *Biomedical Engineering Advances*, *9*, 100141 (article). https://doi.org/10.1016/j.bea.2024.100141

Sauret, A., Ray, T. R., & Compton, B. G. (2026). Fluid Mechanics Challenges in Direct-Ink-Writing Additive Manufacturing. *Annual Reviews*, *58*, 413–442. https://doi.org/10.1146/annurev-fluid-100224-111013

Shi, W., Li, H., Xu, C., Wu, G., Chen, J., Zhang, J., Liang, L., Wu, Q., Liang, Y., Li, G., & Tang, W. (2024). Ag@polydopamine-functionalized borate ester-linked chitosan hydrogel integrates monitoring with wound healing for epidermal sensor. *Npj Flexible Electronics*, *8*, 82. https://doi.org/10.1038/s41528-024-00366-4

Singh, R., Thirumalai, D., Levingstone, T., & Morrin, A. (2026). Towards a wearable format for transducing responsive swelling in hydrogels. *Materials Advances*, *7*(7), 3698–3707. https://doi.org/10.1039/d5ma01115a

Tahir, D., Ardiansyah, A., Heryanto, H., Mhd Noor, E. E., & Mohamed, M. A. (2025). Chitosan-based hydrogels: A comprehensive review of transdermal drug delivery. *International Journal of Biological Macromolecules*, *298*, 140010 (article). https://doi.org/10.1016/j.ijbiomac.2025.140010

Tian, G., Zhu, M., Chen, J., Liang, C., Zhao, Q., Yang, D., Liu, Y., Tang, S., Huang, J., Liu, Z., Lu, W., Zhu, M., Yan, W., & Qi, D. (2025). Anti-fatigue adhesive non-swelling hydrogel constructed by covalent topological structure and micro-nano gel for stretchable bioelectronics. *Bioactive Materials*, *53*, 178–187. https://doi.org/10.1016/j.bioactmat.2025.06.045

Wang, Y., Zhang, X., Zhao, X., Yang, X., Yuan, M., Zheng, Y., Tang, J., Liu, W., Zhang, J., & Lin, L. (2025). Excellent electrochemical performance based on covalently crosslinked chitosan hydrogel electrolytes induced structural stability against alkali. *Advanced Composites and Hybrid Materials*, *8*, 183 (article). https://doi.org/10.1007/s42114-024-01191-z

Wu, S., Wu, S., Zhang, X., Feng, T., & Wu, L. (2023). Chitosan-Based Hydrogels for Bioelectronic Sensing: Recent Advances and Applications in Biomedicine and Food Safety. *Biosensors*, *13*(1), 1–15. https://doi.org/10.3390/bios13010093

Yalamanchili, S. (2011). *Comparison of Standard Impedance Spectroscopy Response to Aqueous Metal Ions Using Plain vs. Surface Derivatized Gold Interdigitated Electrodes* [Eastern Michigan University]. http://commons.emich.edu/theses

Zha, X., Wang, C., Meng, Z., Ye, Y., Sun, H., Tan, C., & Tian, Y. (2026). Intrinsically Thermoresponsive Hydrogels from Molecularly Engineered Chitosan. *Gels*, *12*(2), 1–14. https://doi.org/10.3390/gels12020119

https://doi.org/10.24191/scl.v20i2.9399